

CrystEngComm

Accepted Manuscript



This is an *Accepted Manuscript*, which has been through the Royal Society of Chemistry peer review process and has been accepted for publication.

Accepted Manuscripts are published online shortly after acceptance, before technical editing, formatting and proof reading. Using this free service, authors can make their results available to the community, in citable form, before we publish the edited article. We will replace this *Accepted Manuscript* with the edited and formatted *Advance Article* as soon as it is available.

You can find more information about *Accepted Manuscripts* in the [Information for Authors](#).

Please note that technical editing may introduce minor changes to the text and/or graphics, which may alter content. The journal's standard [Terms & Conditions](#) and the [Ethical guidelines](#) still apply. In no event shall the Royal Society of Chemistry be held responsible for any errors or omissions in this *Accepted Manuscript* or any consequences arising from the use of any information it contains.

Seven entangled coordination polymers assembled from triphenylamine-based bisimidazole and dicarboxylates: interpenetration, self-penetration and mixed entanglement

Xianmin Guo,^a Yongnian Yan,^a Huadong Guo,^{*a} Yanjuan Qi^a and Chunming Liu^{*a}

⁵ Received (in XXX, XXX) Xth XXXXXXXXXX 20XX, Accepted Xth XXXXXXXXXX 20XX

DOI: 10.1039/b000000x

Seven new entangled coordination polymers, namely, [Zn(sdc)(bita)] (1), [Zn(1,4-ndc)(bita)] (2), [Zn₂(bdc)₂(bita)₂] (3), [Zn₂(sda)₂(bita)₂] (4), [Cd(odc)(bita)]·0.5H₂O (5), [Cd₂(bpdc)₂(bita)₂] (6) and [Cd₃(bpdc)₃(bita)₂]·2DMF (7) [bita=4,4'-bisimidazyltriphenylamine, H₂sdc=4,4'-sulfonyldibenzoic acid, 1,4-H₂ndc= naphthalene-1,4-dicarboxylic acid, H₂bdc=1,4-benzenedicarboxylic acid, H₂odc=4,4'-oxybisbenzoic acid, H₂sda= 4,4'-stilbenedicarboxylic acid, H₂bpdc= biphenyl-4,4'-dicarboxylic acid], have been synthesized and structurally characterized. Compound 1 exhibits a 2D→2D polycatenane of three-fold interpenetrated **sql** networks. Compound 2 displays a four-fold interpenetration of **dia** network in a [2+2] mode. Compound 3 features both polyrotaxane and polycatenane comprised of two interlocked sets of **hcb** network. Compound 4 shows a three-fold interpenetration of **pcu** network. Compound 5 presents an unusual two-fold interpenetration of self-penetration framework with (4²·6·8³) topology. Compound 6 displays a 2D→3D polycatenane of three-fold interpenetrated **sql** networks. Compound 7 exhibits an unusual self-penetration framework with (4²⁵·6³) topology. The thermal stabilities and photochemical properties of these compounds have also been studied.

20 INTRODUCTION

The self-assembly of entangled coordination polymers has always been a hot researching issue in the field of supra-molecular chemistry and crystal engineering in recent years, not only because of their interesting structural diversity,¹ but also for their potential applications as functional materials.² The exploitation of these structures can be helpful for both the design and analysis of crystal structures and understanding the relationships between the structure and function of these coordination polymers. Among such systems, interpenetration and self-interpenetration are most investigated types of entanglement.³ The former can be described as a number of individual nets participating in interpenetration with each other. The latter, however, are single nets having the peculiarity that the smallest topological rings are catenated by other rings belonging to the same net. Another fascinating phenomenon contributing much to the topological diversity is the coexistence of different entangled modes in one structure, such as the coexistence of interpenetration and polyrotaxane, the coexistence of polyrotaxane and polycatenane, and so on.⁴ One common feature in these structures is that part of the linkers belong to one net are occupied by the coordinative rings, which are penetrated or catenated by motifs from the mutually entangled nets. However, the mixed entanglements including interpenetration and self-penetration are less reported. It is mainly because that the self-penetration seriously minimizes the void space within the single network, which definitely prevents the interpenetration of other nets.

Although remarkable progress has been made in this field, it is still difficult to synthesize entangled motifs with tailored structures and properties, since a lot of factors, such as the temperature, pH value, solvents and counter anions, can impose unpredictable impact on the final architectures. The rational choice of organic spacers with long size and flexibility has proven to be an effective strategy to generate entangled topologies.⁵ Along with our research on the building of entangled frameworks,⁶ in this paper, we have designed and synthesized a new V-shaped semi-rigid bisimidazole ligand, 4,4'-bisimidazyltriphenylamine (bita), as the building unit, which features three special characteristics: (1) The long size makes it as a reasonable candidate to generate CPs with open frameworks. (2) The free rotation of imidazole rings can promote the flexibility of ligand to meet the requirement of coordination geometries of metal ions for tuning the fine structure. (3) Its bent conformation, especially, is potential to assemble a molecular unit with loops. Meanwhile, to further investigate the influence of dicarboxylate acids on the formation of supra-molecular architectures, a series of dicarboxylic acids with different conformation were introduced (Scheme 1). Successfully, we have synthesized seven new entangled coordination polymers, namely [Zn(sdc)(bita)] (1), [Zn(1,4-ndc)(bita)] (2), [Zn₂(bdc)₂(bita)₂] (3), [Zn₂(sda)₂(bita)₂] (4), [Cd(odc)(bita)]·0.5H₂O (5), [Cd₂(bpdc)₂(bita)₂] (6) and [Cd₃(bpdc)₃(bita)₂]·2DMF (7). These compounds have been characterized by elemental analysis, IR spectroscopy, thermogravimetric analysis (TGA) and X-ray crystallography.

Scheme 1. The building units that were used.

Experimental section

All the other starting materials were of analytic grade and used as received without further purification. Elemental analyses (C, H, N) were performed with a Perkin-Elmer 240c elemental analyzer. TGA was performed on a Perkin-Elmer TG-7 analyzer heated from 30 to

650 °C under nitrogen. The luminescent properties of these compounds were measured on a HITACHI F-7000 spectrometer. IR spectra were obtained from KBr pellets on a Perkin-Elmer 580B IR spectrometer in the 400-4000 cm⁻¹ region.

Synthesis of bita. A mixture of Cu₂O (0.07g, 0.5mmol), 4,4'-dibromotriphenyl amine (4.03g, 10mmol), imidazole (2.72g, 40mmol), and K₂CO₃ (5.52g, 40mmol) in anhydrous DMF (30mL) in a 100mL two-necked round-bottom flask under N₂ was stirred at 150°C for 48 h. The reaction mixture was filtered, and then the filtrate was added into 300mL of H₂O. The deposit was filtered and washed with water and dried in vacuum to afford the product in 50%. Anal. calcd. for C₁₈H₁₃Br₂N (%): C, 53.63; H, 3.25; N, 3.47. Found: C, 53.54; H, 3.32; N, 3.44.

Synthesis of [Zn(sdc)(bita)] (1). A mixture of Zn(OAc)₂·2H₂O (0.0220g, 0.1mmol), H₂sdc (0.0377g, 0.1mmol), bita (0.0332g) and H₂O (10ml) was placed in a Teflon reactor (20ml) and heated at 160°C for 4 days. After gradually cooled to room temperature at a rate of 10°C·h⁻¹, pale crystals of **1** were obtained with 46% yield based on bita. Anal. Calcd for C₃₈H₂₇N₅O₆SZn: C, 61.09; H, 3.64; N, 9.37. Found: C, 60.88; H, 3.40; N, 9.12. IR (KBr, cm⁻¹): 3136 (w), 3069 (w), 1640 (s), 1624 (s), 1593 (w), 1568 (m), 1519 (s), 1488 (s), 1395 (m), 1353 (s), 1318 (s), 1292 (s), 1265 (m), 1241 (m), 1160 (m), 1129 (m), 1101 (s), 1065 (s), 965 (w), 834 (m), 779 (w), 744 (s), 722 (m), 714 (w), 693 (m), 620 (m), 575 (w), 543 (m).

Synthesis of [Zn(1,4-ndc)(bita)] (2). Complex **2** was synthesized following the same synthetic procedure as that for complex **1** except that 1,4-H₂ndc was used instead of H₂sdc. Pale crystals of **2** were obtained with 50% yield based on bita. Anal. Calcd for C₃₆H₂₅N₅O₄Zn: C, 65.81; H, 3.84; N, 10.66. Found: C, 65.68; H, 3.70; N, 10.37. IR (KBr, cm⁻¹): 3131 (m), 3099 (m), 1598 (s), 1559 (s), 1520 (s), 1456 (m), 1398 (s), 1352 (s), 1314 (s), 1262 (s), 1210 (m), 1152 (m), 1119 (m), 1068 (s), 1020 (w), 964 (s), 945 (w), 828 (s), 789 (m), 751 (m), 693 (m), 660 (m), 621 (w), 576 (w), 544 (m).

Synthesis of [Zn₂(bdc)₂(bita)₂] (3). Complex **3** was synthesized following the same synthetic procedure as that for complex **1** except that H₂bdc was used instead of H₂sdc. Pale crystals of **3** were obtained with 42% yield based on bita. Anal. Calcd for C₆₄H₄₆N₁₀O₈Zn₂: C, 63.33; H, 3.82; N, 11.54. Found: C, 63.10; H, 3.99; N, 11.42. IR (KBr, cm⁻¹): 3138 (m), 3105 (w), 1618 (s), 1520 (s), 1489 (s), 1346 (s), 1314 (s), 1275 (s), 1133 (m), 1061 (s), 1010 (w), 964 (m), 887 (w), 822 (s), 751 (s), 700 (m), 654 (m), 621 (w), 589 (w), 551 (m), 518 (m).

Synthesis of [Zn₂(sda)₂(bita)₂] (4). Complex **4** was synthesized following the same synthetic procedure as that for complex **1** except that H₂sda was used instead of H₂sdc. Pale crystals of **4** were obtained with 47% yield based on bita. Anal. Calcd for C₈₀H₅₈N₁₀O₈Zn₂: C, 67.76; H, 4.12; N, 9.88. Found: C, 67.48; H, 4.34; N, 9.60. IR (KBr, cm⁻¹): 3119 (w), 3047 (w), 1618 (s), 1592 (s), 1540 (m), 1515 (s), 1366 (s), 1314 (s), 1262 (s), 1236 (s), 1178 (m), 1133 (m), 1061 (s), 1016 (w), 964 (m), 938 (m), 861 (m), 847 (m), 828 (m), 784 (m), 700 (m), 660 (m), 537 (m).

Synthesis of [Cd(ode)(bita)]·0.5H₂O (5). Complex **5** was synthesized following the same synthetic procedure as that for complex **1** except that H₂ode was used instead of H₂sdc and Cd(OAc)₂·2H₂O was used instead of Zn(OAc)₂·2H₂O. Pale crystals of **5** were obtained with 42% yield based on bita. Anal. Calcd for C₃₈H₂₈CdN₅O_{5.5}: C, 60.44; H, 3.74; N, 9.28. Found: C, 59.52; H, 3.99; N, 9.30. IR (KBr, cm⁻¹): 3112 (w), 3040 (w), 1592 (s), 1515 (s), 1391 (s), 1314 (m), 1268 (s), 1223 (s), 1159 (m), 1119 (m), 1061 (s), 1010 (w), 932 (w), 874 (m), 835 (m), 784 (m), 751 (m), 700 (m), 660 (s), 537 (m).

Synthesis of [Cd₂(bpdC)₂(bita)₂] (6). Complex **6** was synthesized following the same synthetic procedure as that for complex **5** except that H₂bpdC was used instead of H₂ode. Pale crystals of **6** were obtained with 46% yield based on bita. Anal. Calcd for C₇₆H₅₄Cd₂N₁₀O₈: C, 62.52; H, 3.73; N, 9.59. Found: C, 62.77; H, 3.90; N, 9.42. IR (KBr, cm⁻¹): 3112 (w), 1682 (w), 1578 (s), 1515 (s), 1482 (s), 1391 (s), 1307 (m), 1262 (m), 1171 (w), 1119 (w), 1061 (s), 1003 (w), 963 (w), 926 (w), 842 (m), 770 (m), 700 (w), 679 (w), 654 (w), 537 (w), 421 (w).

Synthesis of [Cd₃(bpdC)₃(bita)₂]·2DMF (7). A mixture of Cd(NO₃)₂·4H₂O (0.0308g, 0.1mmol), H₂bpdC (0.0242g, 0.1mmol), bita (0.0377g, 0.1mmol), DMF (8ml) and H₂O (2ml) was placed in a Teflon reactor (20ml) and heated at 80°C for 2 days. After gradually cooled to room temperature, colorless crystals of **7** were obtained with 47% yield based on bita. Anal. Calcd for C₉₆H₇₆Cd₃N₁₂O₁₄: C, 58.86; H, 3.91; N, 8.58. Found: C, 58.70; H, 3.99; N, 8.44. IR (KBr, cm⁻¹): 3131 (m), 3054 (w), 1676 (s), 1585 (s), 1515 (s), 1385 (s), 1307 (s), 1268 (s), 1071 (s), 1119 (s), 1061 (s), 1003 (s), 964 (m), 932 (m), 854 (s), 828 (s), 770 (s), 700 (s), 654 (s), 615 (w), 544 (m), 472 (w), 414 (s).

X-ray Crystallography. Single-crystal XRD data for compounds **1-7** were recorded on a Bruker Apex CCD diffractometer with graphite-monochromatized Mo K α radiation ($\lambda = 0.71073 \text{ \AA}$) at 285(2) K. Absorption corrections were applied using the multiscan technique. All the structures were solved by Direct Method of SHELXS-97⁷ and refined by the full-matrix least-squares techniques by using the SHELXL-97⁸ program within WINGX. No-hydrogen atoms were refined with anisotropic temperature parameters. The hydrogen atoms of the organic ligands were refined as rigid groups. The hydrogen atoms of water molecules in compound **5** are not added. For the high vibration, the disordered C3, C4 and O2 atoms in compound **6**, and the C17, C18, C38, C39 and O6 atoms in compound **7** were refined using C and O atoms split over two sites with a total occupancy of 1 and handled by isotropic refinement. It should be noted that the guest molecules in the channels of **7** are highly disordered and could not be modeled properly so the diffused electron densities resulting from them were removed by the SQUEEZE routine in PLATON.⁹ The detailed crystallographic data and structure refinement parameters for **1-7** are summarized in Table 1.

Table 1. Crystal and Structure Refinement Data for Compounds **1-7**.

Results and discussion

Structure description of 1

Compound **1** crystallizes in a monoclinic space group $P2_1/n$. In the asymmetric unit, there exist one crystallographically unique Zn(II) atom, one sdc^{2-} anion and one coordinated bita ligand. As shown in Fig. 1a, the Zn(II) atom is coordinated by two nitrogen atoms from two different bita ligands (Zn-N 1.982(3)- 2.032(3) Å) and two oxygen atoms from two sdc^{2-} anions (Zn-O 1.927(3)- 1.947(3) Å) to generate a distorted tetrahedral geometry. Zn(II) to O/N distances and bond angles are within the normal range (Table S1 in the supporting information). The sdc^{2-} anion connects two Zn(II) atoms with two monodentate carboxylates. The dihedral angle of two benzyl rings is ca. 105.93°. The bita ligand acts as a linker to bridge two adjacent Zn(II) atoms.

Fig. 1. (a) The coordination environment of Zn(II) atom in **1**. The hydrogen atoms are omitted for clarity. A: $-x+5/2, y+1/2, -z+1/2$; B: $-x-1/2, y-1/2, -z+1/2$. (b) The perspective view of the 2D layer framework. (c) The perspective view of the three different helical chains in **1**. (d) and (e). The perspective and schematic views of the three-fold interpenetration of **sql** network. (Noted: the dangling benzyl rings in b, c and d are omitted for clarity)

In compound **1**, Zn(II) atoms are connected by sdc^{2-} anions and bita ligands to generate a 2D undulated layer (Fig. 1b). Within the layer, the adjacent Zn(II) atoms are separated by distances of 13.30 Å (by sdc^{2-}) and 16.91 Å (through bita). If organic ligands are considered as linkers, Zn(II) atoms can be clarified as four-connected nodes. Thus, the topology of the structure can be simplified as a uninodal (4, 4)-connected **sql** net with point symbol $\{4^4.6^2\}$. Along the direction of b axis, there exist two kinds of helical chains: one constructed from sdc^{2-} anions and metal centers and the other generated from bita and metal centers. Both helices possess a pitch of 18.31 Å corresponding to the length of b axis. While, along the direction of a axis, every one bita and sdc^{2-} are connected by Zn(II) atoms to build another helical chain, with a pitch of 22.43 Å corresponding to the triple length of a axis (Fig. 1c). The potential voids are filled via mutual interpenetration of another two independent equivalent framework in a normal mode, giving rise to a three-fold 2D→2D polycatenane sheet (Fig. 1d and 1e). Each kind of helical chains in one sheet exhibit the uniform hardness, opposite to the ones from neighboring sheets.

Structure description of 2

Compound **2** crystallizes in a monoclinic space group $P21/n$. In the asymmetric unit, there exist one crystallographically unique Zn(II) atom, one 1,4- ndc^{2-} anion and one coordinated bita ligand. As shown in Fig. 2a, the Zn(II) atom is four-coordinated by two nitrogen atoms from two individual bita ligands (Zn-N 1.998(4)-2.010(4) Å) and two oxygen atoms from two 1,4- ndc^{2-} anions (Zn-O 1.924(4)-1.947(4) Å), displaying a slightly distorted tetrahedral geometry. Zn(II) to O/N distances and bond angles are within the normal range (Table S2 in the supporting information). The 1,4- ndc^{2-} anion connects two Zn(II) atoms with two monodentate carboxylates. The bita ligand acts as a linker to join two adjacent Zn(II) atoms.

Fig. 2. (a) The coordination environment of Zn(II) atom in **2**. The hydrogen atoms are omitted for clarity. A: $x+1/2, -y+1/2, z+1/2$; B: $x-1/2, -y-1/2, z+1/2$. (b) The perspective view of the diamondoid network. (c) and (d) The schematic views of the [2+2] interpenetration mode along different directions in **2**. (Noted: the dangling benzyl rings in b are omitted for clarity)

In the structure, each Zn(II) center is linked to four other metal centers by the organic spacers to construct a 3D open framework. The adjoining metal centers are separated by distances that are 10.82 Å (through 1,4- ndc^{2-}) and 16.48 Å (through bita). If the 1,4- ndc^{2-} anions and bita ligands are considered as linkers, and metal centers are considered as four-connected nodes, the architecture can be regarded as a typical 3D diamond framework. A single adamantane cage is illustrated in Fig. 3b, which exhibits a maximum dimension of 39.25 Å × 33.97 Å × 27.99 Å (corresponding to the longest intracage Zn...Zn distances). Because of the spacious nature of the single network, the potential voids are filled via mutual interpenetration of the other three independent equivalent frameworks, generating a four-fold interpenetrating architecture. Unusually, in the case of compound **2**, the interpenetration mode differs from the normal mode and can be described as two sets of 4-fold net, that is, an unusual [2+2] mode of interpenetration. In each set, the independent equivalent cages are separated from each other by 19.63 Å corresponding to the length of b axis. The two sets of 2-fold nets are translationally equivalent with a relative displacement distance of 3.14 Å (Fig. 3c and 3d).

Structure description of 3

Compound **3** crystallizes in a triclinic space group $P-1$. In the asymmetric unit, there exist one crystallographically unique Zn(II) atom, one bita ligand, and two half bdc^{2-} anions lying about independent inversion centres. As shown in Fig. 3a, the Zn(II) atom is ligated by two nitrogen atoms from two bita ligands (Zn-N 1.997(2)-2.006(2) Å) and two oxygen atoms from two bdc^{2-} anions (Zn-O 1.941(2)-1.9667(19) Å), resulting into a tetrahedral geometry. Zn(II) to O/N distances and bond angles are within the normal range (Table S3 in the supporting information). The bdc^{2-} anion connects two Zn(II) atoms with two monodentate carboxylates. The bita ligand acts as a linker to connect two neighboring Zn(II) atoms.

In compound **3**, a pair of bita ligands bridge two adjacent Zn(II) atoms to give a 32-membered ring $[\text{Zn}_2(\text{bita})_2]$ with a dimension of 9.46 Å × 9.58 Å, which is further bridged by bdc^{2-} anions to form a 2D layer motif (Fig. 3b). Topological analysis shows that it is a uninodal (6, 3)-connected **hcb** network with the point symbol $\{6^3\}$, in which each hexagon has four edges represented by the bdc^{2-} anions and two edges replaced by the $[\text{Zn}_2(\text{bita})_2]$ rings (Fig. 3c). The neighboring Zn(II) atoms are separated by distance of 11.06 Å, 11.07 Å (through

bdc²⁻) and 15.60 Å (through bita). In order to minimize the void cavities and stabilize the framework, the potential voids formed by a single 2D network show incorporation of another identical network, thus giving a two-fold parallel interpenetrating sheet. After deep insight into the structure, each [Zn₂(bita)₂] ring in one layer is threaded by the rod bdc²⁻ ligand from the other layer, and vice versa (Figure. 3d). Meanwhile, the terminal phenyl rings of bita in one sheet interdigitate into the hexagons from neighboring sheets above and below, which definitely promote the stability of whole structure (Figure. 3e). So compound **3** presents the coexistence of entanglement in one structure: polyrotaxane and polycatenane (Figure. 3f).

Fig. 3. (a) The coordination environment of Zn(II) atom in **3**. The hydrogen atoms are omitted for clarity. A: -x+2,-y+2,-z. (b) and (c) The perspective and schematic views of the **hcb** network. (d) The perspective view of the rotaxane-like motif in **3**. (e) The perspective view of the catenane-like motif in **3**. (f) The perspective view of polyrotaxane and polycatenane in the 2-fold interpenetration network. (Noted: the dangling benzyl rings in b, d, e and f are omitted for clarity)

Structure description of 4

Compound **4** crystallizes in the monoclinic space group *P2/c*. In the asymmetric unit, there exist one crystallographically unique Zn(II) atom, two half sda²⁻ anions and one bita ligand. As shown in Fig. 5a, the Zn(II) atom is five-coordinated by two nitrogen atoms from two bita ligands (Zn-N 2.044(4)-2.046(3) Å) and three oxygen atoms from two sda²⁻ anions (Zn-O 1.941(3)-2.278(4) Å). Zn(II) to O/N distances and bond angles are within the normal range (Table S5 in the supporting information). One sda²⁻ anion connects two Zn(II) atoms with two monodentate carboxylates; and the other sda²⁻ anion links two Zn(II) atoms with two chelate carboxylates. The bita ligand acts as a bridge to join two neighboring Zn(II) atoms.

In compound **4**, Zn(II) atoms are connected by bita ligands to generate 1D helical chains. If bita ligands are omitted, the Zn(II) atoms are combined by sda²⁻ anions to assemble 1D meso-helix (Fig. 4b). The whole structure presents a 3D polymeric framework. Within the framework, the neighboring Zn(II) atoms are separated by distance of 17.42 Å (by sda²⁻) and 15.87 Å sda²⁻ (through bita). From the viewpoint of network topology, Zn(II) atoms can be regarded as four-connected nodes and organic ligands as linkers (Fig. 4c). Thus, the resulting structure presents a uninodal 3D network with a schläfli symbol of (4²·6·8³), representing a new topological prototype (Fig. 4d). Notably, this net displays a self-penetrating pattern, within which two of the shortest 4-membered circuits (including four Zn(II) atoms and four sda²⁻ anions) and 8-membered circuits (including eight Zn(II) atoms, four sda²⁻ anions and four bita ligands) are penetrated with each other, which are further connected by sharing one of sda²⁻ linkages (Fig. 4e). The potential voids are large enough to be filled via mutual interpenetration of another independent equivalent framework, generating a two-fold interpenetrating 3D architecture (Fig. 4f). So compound **4** presents the coexistence of entanglement in one structure: interpenetration and self-penetration.

Fig. 4. (a) The coordination environment of Zn(II) atom in **4**. The hydrogen atoms are omitted for clarity. A: x-1,y-1,z; B: x+1,y+1,z. (b) The perspective view of the helical chains in **4**. (c) The perspective view of the 4-connected node. (d) The schematic view of the single self-penetrating network with (4²·6·8³) topology. (e) The schematic view of the self-penetrating motif in **4**. (f) The schematic view of the 2-fold interpenetration framework of two equivalent self-penetration net. (Noted: the dangling benzyl rings in b and c are omitted for clarity)

Structure description of 5

Compound **5** crystallizes in the monoclinic space group *C2/c*. In the asymmetric unit, there exist one crystallographically unique Cd(II) atom, one odc²⁻ anion, one bita ligand and half an uncoordinated water molecule. As shown in Fig. 4a, the Cd(II) atom is five-coordinated by two nitrogen atoms from two bita ligands (Cd-N 2.265(2)-2.339(3) Å) and three oxygen atoms from two odc²⁻ anions (Cd-O 2.1695(19)-2.556(2) Å). Cd(II) to O/N distances and bond angles are within the normal range (Table S4 in the supporting information). The odc²⁻ anion connects two Cd(II) atoms with one monodentate carboxylate, and one chelate carboxylate. The bita ligand acts as a linker to connect two neighboring Cd(II) atoms.

In compound **5**, if the weak secondary bond Cd1...O4A (2.671 Å) is calculated, Cd1 and its symmetry-related Cd1A are bridged by O4A and O4B to form a binuclear Cd₂ cluster. The adjacent clusters are connected by bita ligands to generate 2D square-grid (4,4) layers (Fig. 5b). These layers are pillared by odc²⁻ anions into an extended 3D open framework. Within the framework, the neighboring Cd₂ clusters are separated by distances of 19.27 Å (through bita) and 15.35 Å (by odc²⁻). If the Cd₂ cluster are considered as six-connected nodes (Fig. 5c), and organic ligands as linkages, topological analysis reveals that compound **5** forms a uninodal six-connected **pcu** net with the point symbol (4¹²·6³) (Fig. 5d). The potential voids are large enough to be filled via mutual interpenetration of other two independent equivalent frameworks, generating a three-fold interpenetrating 3D architecture (Fig. 5e).

Fig. 5. (a) The coordination environment of Cd(II) atom in **5**. The hydrogen atoms are omitted for clarity. A: x+1,-y,z+1/2; B: x+1/2,-y+1/2,z-1/2. (b) The perspective view of the 2D undulated grid (4, 4) layer built from the Cd₂ clusters and bita ligands. (c) The perspective view of the 6-connected node. (d) The perspective view of the 3D single framework. (e) The schematic view of three-fold interpenetration of **pcu** network. (Noted: the dangling benzyl rings in b, c and d are omitted for clarity)

Structure description of 6

Compound **6** crystallizes in the monoclinic space group $P-1$. In the asymmetric unit, there exist one crystallographically unique Cd(II) atom, one bita ligand, and two half bpdc^{2-} anions lying about independent inversion centres. As shown in Fig. 6a, the Cd(II) atom is ligated by two nitrogen atoms from two bita ligands (Cd-N 2.235(3)-2.374(4) Å) and three oxygen atoms from two bpdc^{2-} anions (Cd-O 2.227(3)-2.397(7) Å). Cd(II) to O/N distances and bond angles are within the normal range (Table S6 in the supporting information). One bpdc^{2-} anion connects two Cd(II) atoms with two monodentate carboxylates; and the other bpdc^{2-} anion links two Cd(II) atoms with two chelate carboxylates. The bita ligand acts as a linker to connect two neighboring Cd(II) atoms. It should be noted the bond distances of $\text{Cd1}\cdots\text{O1A}$ (2.796 Å) and $\text{Cd1}\cdots\text{O4}$ (2.663 Å) are shorter than the sum of the van der Waals radii, which indicates a weak secondary bonding. This phenomenon may contribute to the distortion of the Cd(II) tetrahedral geometry and result in the variation of coordination environment.

In compound **6**, if the weak secondary bonding is not calculated, the Cd(II) atoms are connected by the organic ligands to generate a 2D zigzag framework. Within the framework, the neighboring Cd(II) atoms are separated by distances of 15.53 Å, 15.57 Å (by bpdc^{2-}) and 16.49 Å (through bita). Topologically, Cd(II) atoms can be regarded as four-connected nodes and organic ligands as linkers (Fig. 6b), thus this layer displays a uninodal (4, 4)-connected **sql** net. Because of the large voids and high undulation, each net entangles with two identical ones from above and below to give a 2D→3D polycatenane framework (Fig. 6c and 6d). While, if the weak secondary bonding is taken into account, Cd1 and its symmetry-related Cd1A are bridged by O1A to form a binuclear Cd_2 dimer. These dimers are linked by the organic ligands to assemble a 3D single framework. Within the framework, the neighboring dimers are separated by distances of 14.24 Å, 17.45 Å (by bpdc^{2-}) and 16.49 Å (through bita). Based on the concept of topology, the Cd_2 dimers can be simplified as six-connected nodes (Fig. 6e), and the organic ligands can be regarded linkers. Thus, the whole structure can be classified into a uninodal six-connected **pcu** net (Fig. 6f).

Fig. 6. (a) The coordination environment of Cd(II) atom in **6**. The hydrogen atoms are omitted for clarity. A: x,y,z-1. (b) The perspective view of the 4-connected node (not calculating the weak secondary bonding). (c) and (d) The perspective and schematic views of the 2D→3D polycatenane framework (not calculating the weak secondary bonding). (e) The perspective view of the 6-connected node (calculating the weak secondary bonding). (f) The schematic view of the **pcu** network (calculating the weak secondary bonding). (Noted: the dangling benzyl rings in b, c and e are omitted for clarity)

Structure description of **7**

Compound **7** crystallizes in a triclinic space group $P-1$. In the asymmetric unit, there exist one and a half Cd(II) atoms, one bita ligand, and three half bpdc^{2-} anions lying about independent inversion centres. As shown in Fig. 7a, the Cd1 atom is in a general position in the unit cell and six-coordinated by one nitrogen atom from one bita ligand (Cd-N 2.2647 Å) and five oxygen atoms from three different bpdc^{2-} anions (Cd-O 2.2025-2.4484 Å) to give a high-distorted octahedral geometry; while, the Cd2 atoms which lies on an inversion centre, is also in a distorted octahedral geometry ligated by two nitrogen atoms from two bita ligands (Cd-N 2.2271 Å) and four oxygen atoms from four bpdc^{2-} anions (Cd-O 2.3717-2.3885 Å). Cd(II) to O/N distances and bond angles are within the normal range (Table S7 in the supporting information). The three bpdc^{2-} anions adopt different coordination modes: one connects two Cd(II) atoms by two chelate carboxylates; one bridges four Cd(II) atoms through two *syn,syn*- μ_2 carboxylates; another links four Cd(II) atoms through two *syn,anti*- μ_2 carboxylates. The bita ligand acts as a linker to join two Cd(II) atoms.

In compound **7**, the Cd2 atom bridges to two neighboring Cd1 atoms by two *syn,syn*- μ_2 carboxylates and two *syn,anti*- μ_2 carboxylates to afford a linear Cd_3 cluster, with the $\text{Cd1}-\mu_2-\text{O1}-\text{Cd2}$ angle of 115.06° and $\text{Cd1}\cdots\text{Cd2}$ distance of 4.08 Å. These clusters are connected by organic ligands to assemble a 3D framework. Within the framework, the adjacent clusters are separated by distance of 13.38 Å, 15.64 Å, 20.37 Å (by bpdc^{2-}) and 17.58 Å (through bita). Based on the concept of topology, the Cd_3 clusters can be regarded as eight-connected nodes, the organic ligands can be regarded as linear linkers, thus the whole structure can be simplified into a uninodal eight-connected network with a schläfli symbol of $(4^{25}.6^3)$ (Fig. 7b and 7c). Further analysis of this structure indicates that it presents a self-penetrating pattern (Fig. 7d). In order to clearly understand such a complicated architecture, the bita ligands are omitted, thus the nodes are joined by bpdc^{2-} anions to give rise to a **pcu** net. As shown in Fig. 7e, along the direction of *b* axis, two neighboring cubic cages combine together to build a new elongated cuboid, in which, the two nodes that locate at the diagonal ends of (1, 1, 0) plane, are bridged by two bita ligands to give a coordinative ring [$\text{Cd}_3(\text{bita})_2\text{Cd}_3$]. These rings are further threaded by the rod bpdc^{2-} anions from the same net to form an unprecedented rotaxane-like self-penetrating motif.

Fig. 7. (a) The coordination environment of Cd(II) atom in **7**. The hydrogen atoms are omitted for clarity. A: -x+1,-y+1,-z. (b) and (c) The perspective and schematic views of the 8-connected node. (d) The perspective view of the self-penetrating motif in **7**. (e) The schematic view of the self-penetrating framework with $(4^{25}.6^3)$ topology.

As shown above, the simultaneous use of bita and six aromatic dicarboxylic ligands afforded seven entangled coordination polymers of interesting architectures. In these compounds, bita ligands adopt similar μ_2 -bridging coordination modes to connect two metal centers, slightly differed by their spatial orientations with respect to the angles of central nitrogen atom and the coordinated nitrogen atoms of the imidazole groups. The carboxylate anions act as key roles in determining the metal nuclearity and hence influencing the connectivity and entanglement of the resulting frameworks (Fig. S4 in the ESI). In compounds **1-4**, the carboxylate groups adopt the monodentate or chelate coordination modes, so that the metal atoms exist only in mono-nuclear fashions. In these compounds, the metal centers are

connected by the carboxylate anions into 1D chains. For compounds **1-3**, the metal centers are also connected by bita to generate another 1D chains, thus the whole structures show four-connected frameworks; while, for compound **4**, the metal centers are combined by bita into 0D coordinative rings, which results into a three-connected network. Obviously, from these four compounds, it is clear that the introduction of different substituted groups to the dicarboxylic acids, varied from the length, size and shapeness, can definitely influence the final supramolecular architectures of the complexes. In compound **5** and **6**, with the presentation of weak secondary bonding, two Cd atoms are bridged together into binuclear clusters, which act as six-connected nodes and further are connected by organic ligands into six-connected networks. In compound **7**, both carboxylate groups adopt bidentate coordination modes, which is attributed to the combination of trinuclear metal clusters and the generation of a specific framework with a high eight-connectivity. On the basis of the synthetic conditions of **6** and **7**, the different solvent molecules have a great influence on the network topologies through the coordination environments of Cd²⁺ and linking modes of bpdc²⁻. Meanwhile, it should be noted that the structural divergence also comes from the different coordination capacity of Zn²⁺ and Cd²⁺, as shown that the latter has more flexible coordination ability to the aggregation of metal ions into multi-nuclear clusters.

Thermal Analysis. To characterize the thermal stabilities of compounds **1-7**, their thermal behaviors were investigated by TGA (Fig. S2 in the ESI). The experiments were performed on samples consisting of numerous single crystals of **1-7** under nitrogen atmosphere with a heating rate of 10°C/min. For **1**, the destruction of the framework occurs at ca. 320°C. The remaining weight corresponds to the formation of ZnO (obsd 10.6%, calcd 10.9%). Compound **2** remains stable up to ca. 300°C, finally leading to the formation of the stoichiometric amount of ZnO as residue (obsd 13.1%, calcd 12.4%). For **3**, the decomposition of the compound occurs at ca. 320°C, and the remaining weight corresponds to the formation of ZnO (obsd 14.3%, calcd 13.4%). Compound **4** is stable up to ca. 360°C with the remaining residue of ZnO (obsd 11.3%, calcd 11.5%). For **5**, the weight loss in the range of 25–130 °C is ascribed to the departure of free water molecules (obsd 2.2%, calcd 1.2%). The decomposition of the framework occurs at ca. 350 °C. The remaining weight corresponds to the formation of CdO (obsd 17.3%, calcd 17.0%). For **6**, the decomposition of the framework occurs at ca. 310 °C. The remaining weight corresponds to the formation of CdO (obsd 17.9%, calcd 17.6%). For **7**, the weight loss in the range of 25–140 °C is attributed to the release of uncoordinated DMF molecules (obsd 7.4%, calcd 7.5%). The whole framework decomposed at ca. 340 °C. The remaining weight corresponds to the formation of CdO (obsd 19.5%, calcd 19.7%).

Photoluminescence Properties. Because of the excellent luminescent properties of d¹⁰ metal coordination polymers and triphenylamine-based compounds,¹⁰ the solid-state luminescence of **1-7** and free bita ligand was investigated at room temperature (Fig. 8 and Table 2). Compound **1** shows a broad band with a peak at 470 nm upon excitation at 367 nm. Compound **2** shows a peak at 397 nm upon excitation at 369 nm. Compound **3** shows a sharp peak at 397 nm excitation at 369 nm. Compound **4** shows a broad peak at 452 nm upon excitation at 398 nm. Compound **5** shows a peak at 390 nm upon excitation at 359 nm. Compound **6** shows a broad peak at 402 nm upon excitation at 331 nm. Compound **7** shows a broad band with a peak at 479 nm upon excitation at 369 nm. Since Zn²⁺ and Cd²⁺ are difficult to oxidize or to reduce due to their d¹⁰ configuration, these emission bands are neither metal-to-ligand charge transfer (MLCT) nor ligand-to-metal transfer (LMCT) in nature.¹¹ For **2, 3, 5** and **6**, the emissions can be essentially ascribed to the luminescence of bita ligand, since a similar emission was observed in the free bita ligand, which shows a band at 398 nm upon excitation at 369 nm. While, for **1, 4** and **7**, in compasion to the luminescence of related dicarboxylic acids and bita (Fig. S3), the emissions can be essentially ascribed to intraligand or ligand-to ligand charge transfer (LLCT). The above observations suggest that these thermally stable polymeric materials may be suitable candidates for potential photoactive materials.

Table 2. Wavelengths of the emission maxima and excitation (nm) for **1-7** and free ligand bita.

Fig. 8. Emission spectra of **1-7** and bita at room temperature.

CONCLUSIONS

In this study, seven new coordination polymers with entangled architectures have been synthesized and characterized using a triphenylamine-based bisimidazole and polycarboxylate acids of versatile conformations. The result of this study demonstrates that the rational selection of organic ligands with specific conformation and geometry is an effective approach to the construction of entangled motifs. These seven compounds not only fill the aesthetic diversity of coordinative network chemistry, but also may provide a potential way to the selective design of versatile network-based materials.

Acknowledgements

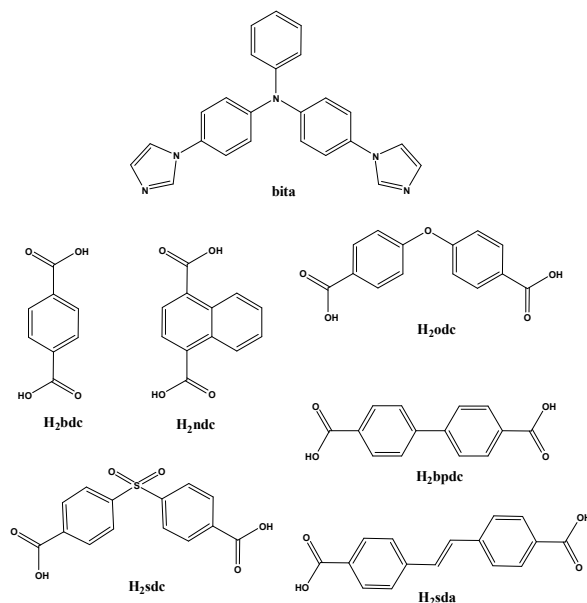
The authors gratefully acknowledge the financial support for this work from the National Natural Science Foundation of China (No. 21101016), the Science Foundation of Jilin Province (No. 20140101038JC and 20140101121JC) and Science Foundation of Changchun Normal University.

Notes and references

^a Department of Chemistry, Changchun Normal University, Changchun, 130032, P. R. China. Fax: +86-431-86168210; Tel: +86-431-86168210; E-mail: hdxmguo@163.com

† Electronic Supplementary Information (ESI) available: [XRD, TGA, CCDC: 1432676-1432682]. See DOI: 10.1039/b000000x/

- 1 (a) O. R. Evans and W. B. Lin, *Acc. Chem. Res.*, 2002, **35**, 511; (b) N. W. Ockwig, O. Delgado-Friederichs, M. O’Keeffe and O. M. Yaghi, *Acc. Chem. Res.*, 2005, **38**, 176; (c) J. P. Zhang, Y. Y. Lin, W. X. Zhang and X. M. Chen, *J. Am. Chem. Soc.*, 2005, **127**, 14162; (d) L. Carlucci, G. Ciani, D. M. Proserpio, T. G. Mitina and V. A. Blatov, *Chem. Rev.*, 2014, **114**, 7557.
- 2 (a) P. Pachfule, Y. F. Chen, J. W. Jiang and R. Banerjee, *J. Mater. Chem.*, 2011, **21**, 17737; (b) J. R. Li, J. Sculley and H. C. Zhou, *Chem. Rev.*, 2012, **112**, 869; (c) O. K. Farha and J. T. Hupp, *Acc. Chem. Res.*, 2010, **43**, 1166; (d) B. L. Chen, S. C. Xiang and G. D. Qian, *Acc. Chem. Res.*, 2010, **43**, 1115; (e) H. Wu, J. Yang, Z. M. Su, S. R. Batten and J. F. Ma, *J. Am. Chem. Soc.*, 2011, **133**, 11406; (f) Z. J. Lin, J. Lü, M. C. Hong and R. Cao, *Chem. Soc. Rev.*, 2014, **43**, 5867.
- 3 (a) V. A. Blatov, L. Carlucci, G. Ciani and D. M. Proserpio, *CrystEngComm*, 2004, **6**, 377; (b) L. Carlucci, G. Ciani and D. M. Proserpio, *Coord. Chem. Rev.*, 2003, **246**, 247; (c) S. R. Batten, *CrystEngComm*, 2001, **3**, 67; (d) X. L. Wang, C. Qin, E. B. Wang and Z. M. Su, *Chem.-Eur. J.*, 2006, **12**, 2680; (e) Y. Qi, Y. X. Che and J. M. Zheng, *Cryst. Growth Des.*, 2008, **8**, 3602; (f) X. J. Ke, D. S. Li, M. Du, *Inorg. Chem. Commun.*, 2011, **14**, 788.
- 15 4 (a) J. Yang, J. F. Ma and S. R. Batten, *Chem. Commun.*, 2012, **48**, 7899; (b) C. Qin, X. L. Wang, E. B. Wang and Z. M. Su, *Inorg. Chem.*, 2008, **47**, 5555; (c) X. Y. Cao, Y. G. Yao, S. R. Batten, E. Ma, Y. Y. Qin, J. Zhang, R. B. Zhang and J. K. Cheng, *CrystEngComm*, 2009, **11**, 1030; (d) Z. G. Gu, X. X. Xu, W. Zhou, C. Y. Pang, F. F. Bao and Z. J. Li, *Chem. Commun.*, 2012, **48**, 3212; (e) X. L. Zhang, C. P. Guo, Q. Y. Yang, W. Wang, W. S. Liu, B. S. Kang and C. Y. Su, *Chem. Commun.*, 2007, 4242.
- 5 (a) H. D. Guo, X. M. Guo, S. R. Batten, J. F. Song, S. Y. Song, S. Dang, G. L. Zheng, J. K. Tang and H. J. Zhang, *Cryst. Growth Des.*, 2009, **9**, 1394; (b) H. D. Guo, X. M. Guo, X. Wang, G. H. Li, Z. Y. Guo, S. Q. Su and H. J. Zhang, *CrystEngComm*, 2009, **11**, 1509; (c) X. M. Guo, H. D. Guo, H. Y. Zou, Y. J. Qi and R. Z. Chen, *CrystEngComm*, 2013, **15**, 9112; (d) H. Wang, F. Y. Yi, S. Dang, W. G. Tian, Z. M. Sun, *Cryst. Growth Des.*, 2013, **14**, 147; (e) M. Du, X. J. Jiang and X. J. Zhao, *Inorg. Chem.*, 2007, **46**, 3984; (f) P. Wang, J. P. Ma, Y. B. Dong and R. Q. Huang, *J. Am. Chem. Soc.*, 2007, **129**, 10620.
- 25 6 (a) H. D. Guo, X. M. Guo, H. Y. Zou, Y. J. Qi and R. Z. Chen, *CrystEngComm*, 2014, **16**, 2176; (b) H. D. Guo, Y. N. Yan, X. M. Guo, H. Y. Zou, Y. J. Qi and C. M. Liu, *CrystEngComm*, 2014, **16**, 10245; (c) H. D. Guo, X. M. Guo, H. Y. Zou, Y. J. Qi, R. Z. Chen, L. Zhao and C. M. Liu, *CrystEngComm*, 2014, **16**, 7459; (d) H. D. Guo, Y. N. Yan, N. Wang, X. M. Guo, G. L. Zheng and Y. J. Qi, *CrystEngComm*, 2015, **17**, 6512.
- 7 G. M. Sheldrick, SHELXS-97, Programs for X-ray Crystal Structure Solution; University of Göttingen: Göttingen, Germany, 1997.
- 8 G. M. Sheldrick, SHELXL-97, Programs for X-ray Crystal Structure Refinement; University of Göttingen: Göttingen, Germany, 1997.
- 9 A.L. Spek, *Acta Cryst.*, C71, 2015, 9-18.
- 30 10 (a) C. M. Angels, J. J. Novoa and S. Alvarez, *J. Am. Chem. Soc.*, 2004, **126**, 465; (b) H. Y. Chao, W. Lu, Y. Q. Li, M. W. Chan, C. M. Che, K. K. Cheung and N. Y. Zhu, *J. Am. Chem. Soc.*, 2002, **124**, 14696; (c) C. D. Wu, H. L. Ngo and W. B. Lin, *Chem. Commun.*, 2004, 1588; (d) J. G. Lin, S. Q. Zang, Z. F. Tian, Y. Z. Li, Y. Y. Xu, H. Z. Zhu and Q. J. Meng, *CrystEngComm*, 2007, **9**, 915; (e) M. D. Allendorf, C. A. Bauer, R. K. Bhakta and R. J. T. Houk, *Chem. Soc. Rev.*, 2009, **38**, 1330; (f) J. Heine and K. Müller-Buschbaum, *Chem. Soc. Rev.*, 2013, **42**, 9232.
- 11 (a) Y. Yang, J. Yang, P. Du, Y. Y. Liu and J. F. Ma, *CrystEngComm*, 2014, **16**, 6380; (b) B. Q. Song, C. Qin, Y. T. Zhang, X. S. Wu, H. S. Liu, K. Z. Shao and Z. M. Su, *CrystEngComm*, 2015, **17**, 3129; (c) H. Wu, J. F. Ma, Y. Y. Liu, J. Yang and H. Y. Liu, *CrystEngComm*, 2011, **13**, 7121.
- 35



Scheme 1. The building units that were used.

5 **Table 1.** Crystal and Structure Refinement Data for Compounds 1-7.

param	1	2	3	4	5	6	7
formula	C ₃₈ H ₂₇ N ₂ O ₆ SZn	C ₃₆ H ₂₈ N ₂ O ₄ Zn	C ₆₄ H ₄₆ N ₁₀ O ₈ Zn ₂	C ₈₀ H ₅₈ N ₁₀ O ₈ Zn ₂	C ₃₈ H ₂₈ CdN ₂ O _{5.5}	C ₇₆ H ₅₄ Cd ₂ N ₁₀ O ₈	C ₉₆ H ₇₆ Cd ₃ N ₁₂ O ₁₄
fw	747.08	656.98	1213.85	1418.10	755.05	1460.09	1958.89
space group	<i>p21/n</i>	<i>p21/n</i>	<i>p-1</i>	<i>p2/c</i>	<i>c2/c</i>	<i>p-1</i>	<i>p-1</i>
a	7.4761(5) Å	12.2467(19)	10.015(7)	12.4152(9)	16.8782(7)	9.7159(19)	9.8926(16)
b	18.3130(14)	19.625(3)	11.864(9)	9.8806(7)	21.3492(9)	11.154(2)	13.378(2)
c	25.1258(18)	13.998(2)	12.319(9)	27.299(2)	20.0506(11)	16.493(3)	19.747(3)
α (deg)	90	90	98.310(14)	90	90	72.729(3)	97.526(3)
β (deg)	93.708(2)	97.063(4)	99.091(14)	97.276(2)	112.1970(10)	78.866(4)	100.724(3)
γ (deg)	90	90	91.291(14)	90	90	85.786(4)	97.005(3)
V	3432.8(4)	3338.7(9)	1428.5(18)	3321.8(4)	6689.5(5)	1674.4(5)	2516.7(7)
Z	4	4	1	2	8	1	1
D _{calcd} (g cm ⁻³)	1.446	1.307	1.411	1.418	1.499	1.448	1.196
F(000)	1536	1352	624	1464	3104	740	912
GOF on F ²	0.989	0.987	1.106	1.035	1.119	1.080	1.025
R ₁ /wR ₂ [I ≥ 2σ(I)]	0.0521/0.1112	0.0687/0.1879	0.0383/0.0976	0.0545/0.1286	0.0315/0.0825	0.0459/0.1240	0.0609/0.1801
R ₁ /wR ₂ (all data)	0.1323/0.1518	0.1544/0.2451	0.0606/0.1168	0.1373/0.1844	0.0561/0.1132	0.0734/0.1509	0.0857/0.1905

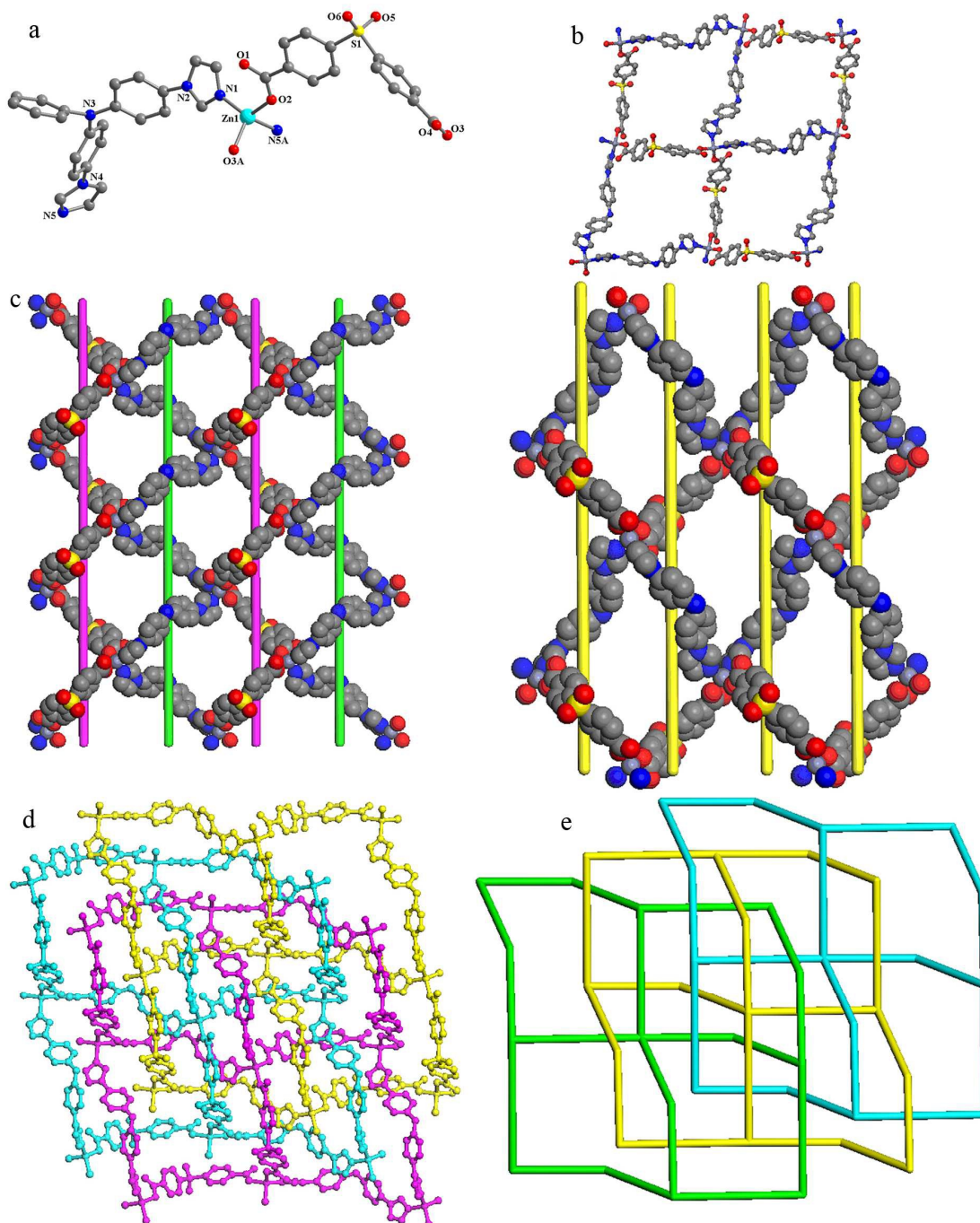


Fig. 1. (a) The coordination environment of Zn(II) atom in **1**. The hydrogen atoms are omitted for clarity. A: $-x+5/2, y+1/2, -z+1/2$; B: $-x-1/2, y-1/2, -z+1/2$.
 (b) The perspective view of the 2D layer framework. (c) The perspective view of the three different helical chains in **1**. (d) and (e). The perspective and
 5 schematic views of the three-fold interpenetration of **sql** network. (Noted: the dangling benzyl rings in b, c and d are omitted for clarity)

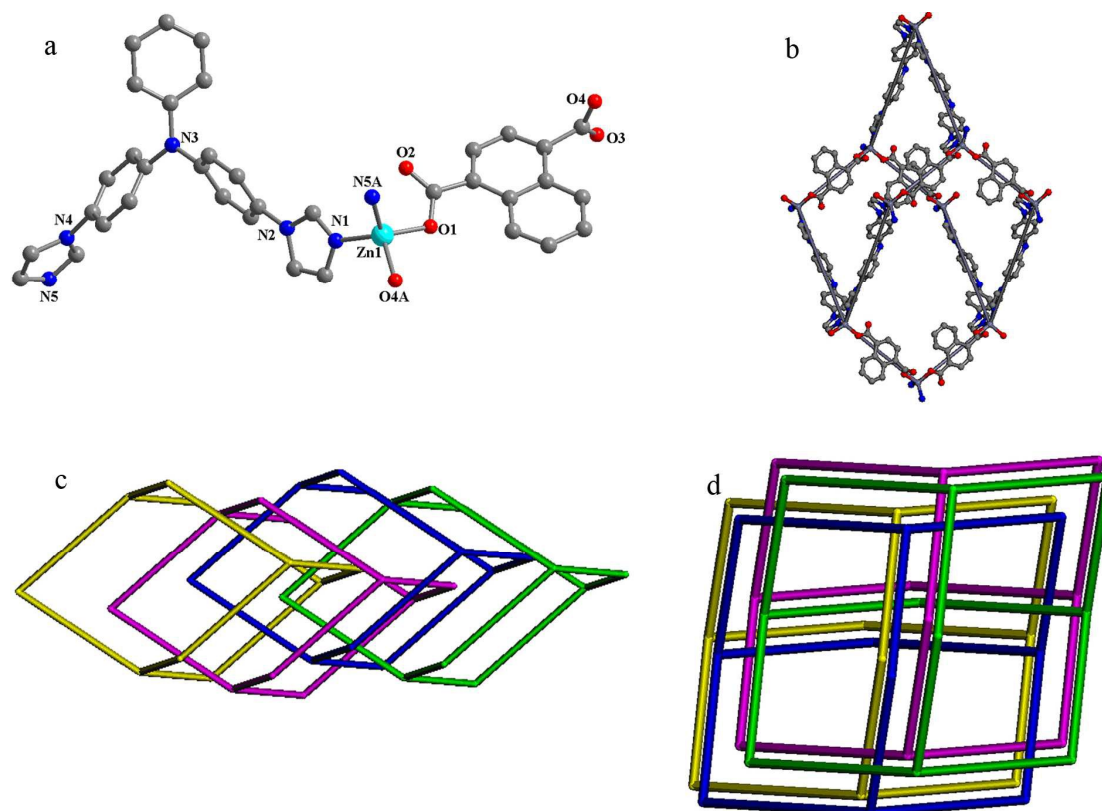


Fig. 2. (a) The coordination environment of Zn(II) atom in **2**. The hydrogen atoms are omitted for clarity. A: $x+1/2, -y+1/2, z+1/2$; B: $x-1/2, -y-1/2, z+1/2$. (b) The perspective view of the diamondoid network. (c) and (d) The schematic views of the [2+2] interpenetration mode along different directions in **2**. (Noted: the dangling benzyl rings in b are omitted for clarity)

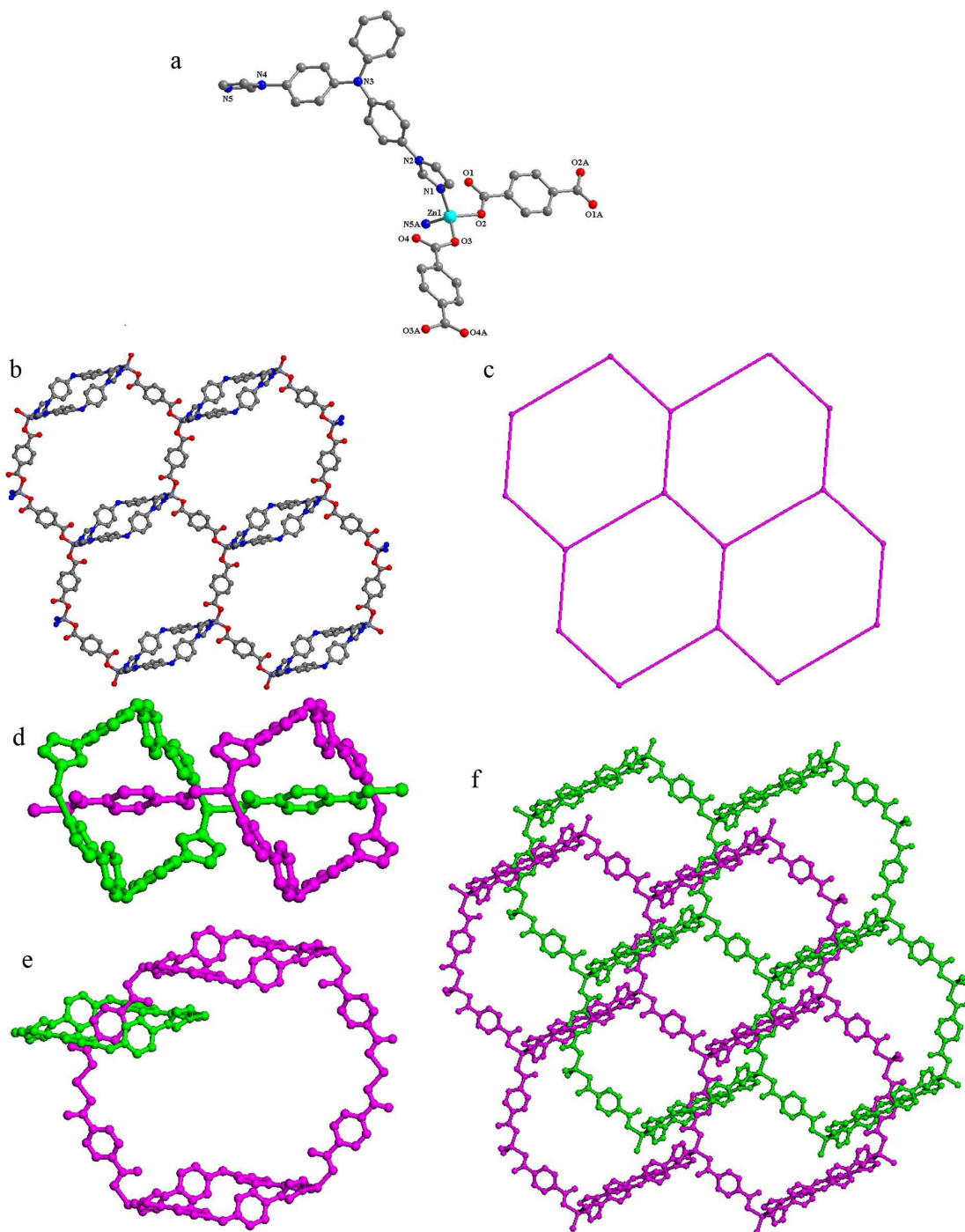


Fig. 3. (a) The coordination environment of Zn(II) atom in **3**. The hydrogen atoms are omitted for clarity. A: $-x+2,-y+2,-z$. (b) and (c) The perspective and schematic views of the **hcb** network. (d) The perspective view of the rotaxane-like motif in **3**. (e) The perspective view of the catenane-like motif in **3**. (f) The perspective view of polyrotaxane and polycatenane in the 2-fold interpenetration network. (Noted: the dangling benzyl rings in b, d, e and f are omitted for clarity)

5

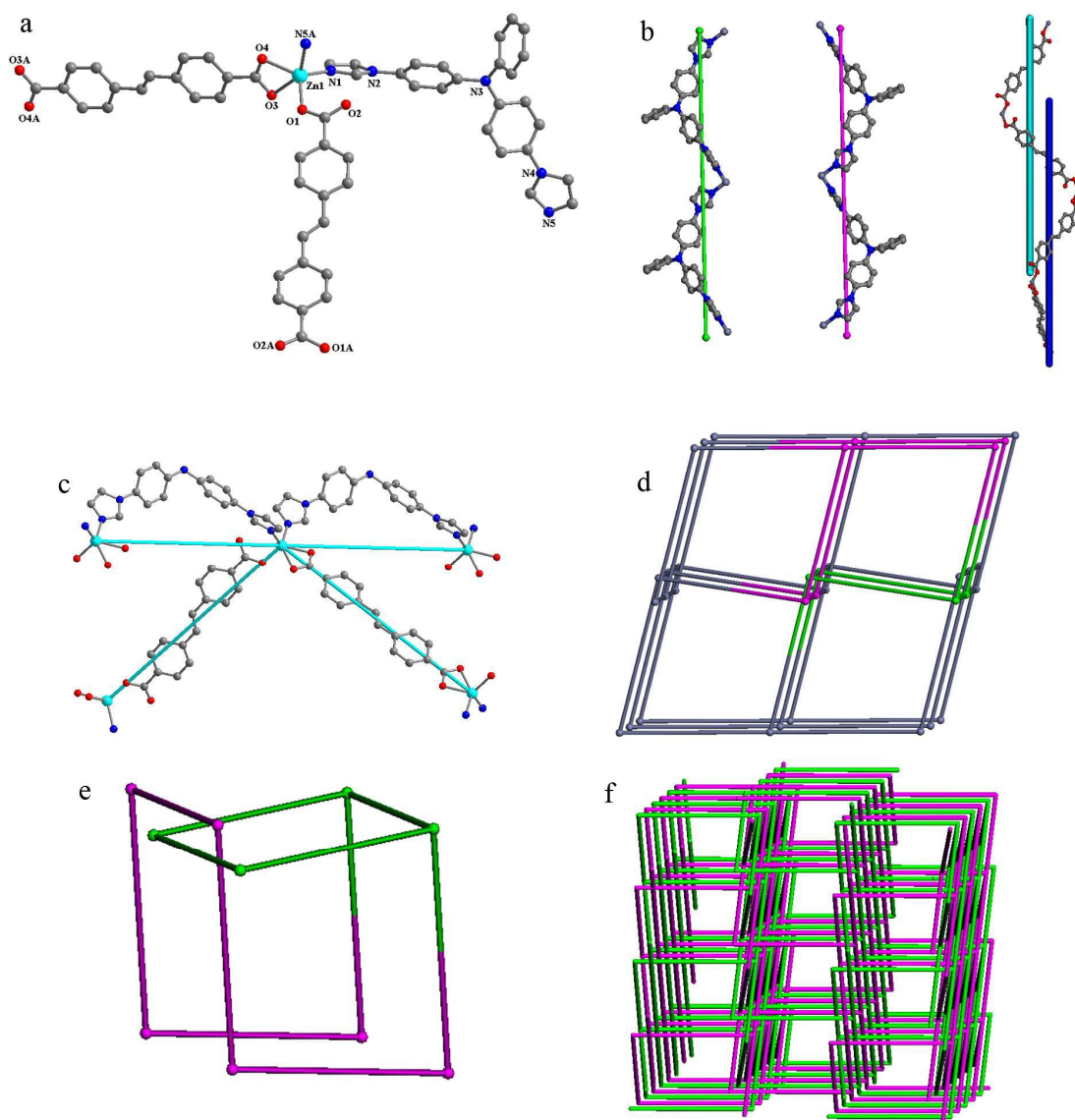


Fig. 4. (a) The coordination environment of Zn(II) atom in **4**. The hydrogen atoms are omitted for clarity. A: $x-1, y-1, z$; B: $x+1, y+1, z$. (b) The perspective view of the helical chains in **4**. (c) The perspective view of the 4-connected node. (d) The schematic view of the single self-penetrating network with (4^2-6-8^3) topology. (e) The schematic view of the self-penetrating motif in **4**. (f) The schematic view of the 2-fold interpenetration framework of two equivalent self-penetrating net. (Noted: the dangling benzyl rings in b and c are omitted for clarity)

5

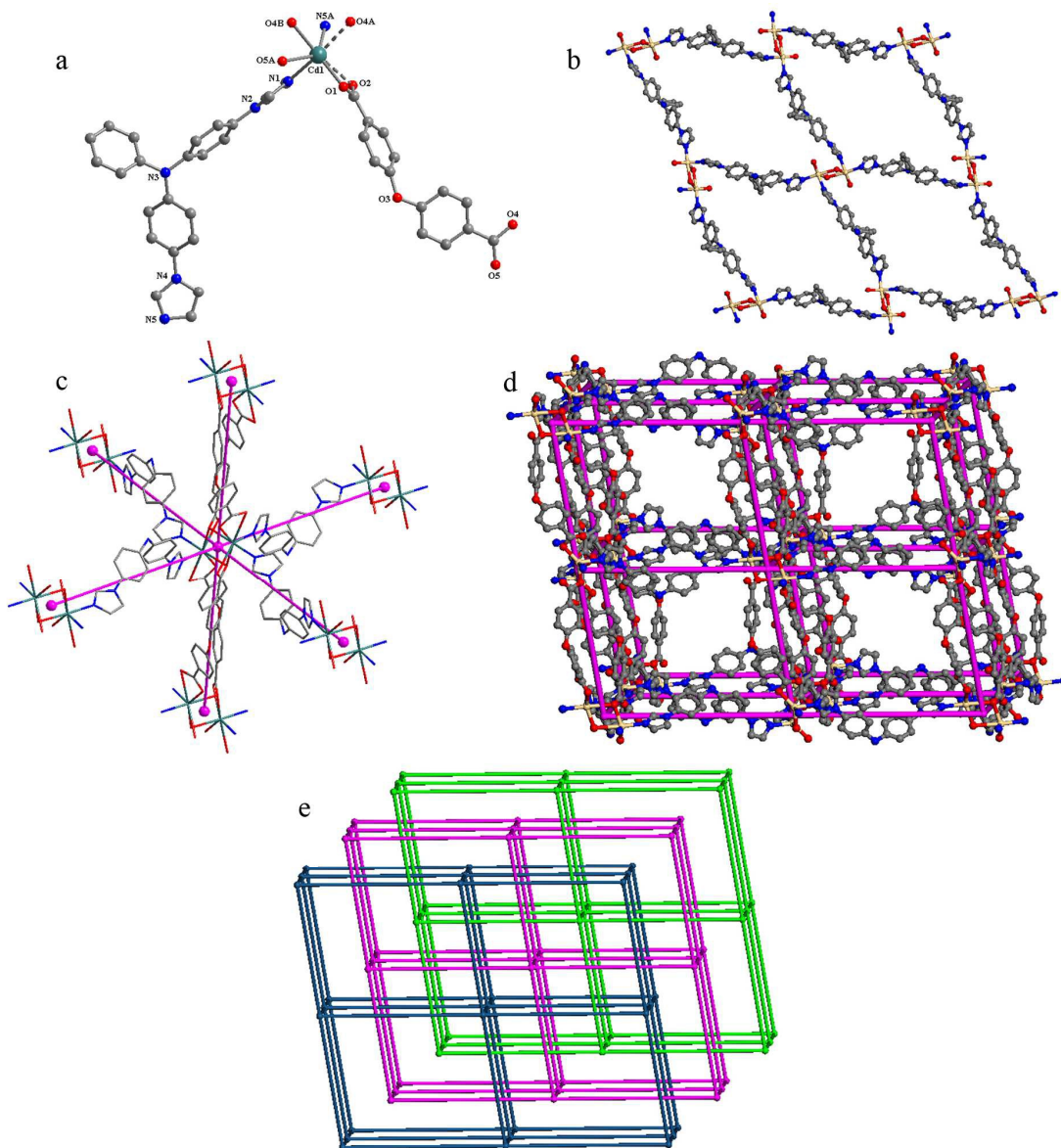


Fig. 5. (a) The coordination environment of Cd(II) atom in **5**. The hydrogen atoms are omitted for clarity. A: $x+1, -y, z+1/2$; B: $x+1/2, -y+1/2, z-1/2$. (b) The perspective view of the 2D undulated grid (4, 4) layer built from the Cd_2 clusters and bita ligands. (c) The perspective view of the 6-connected node. (d) The perspective view of the 3D single framework. (e) The schematic view of three-fold interpenetration of **pcu** network. (Noted: the dangling benzyl rings in b, c and d are omitted for clarity)

5

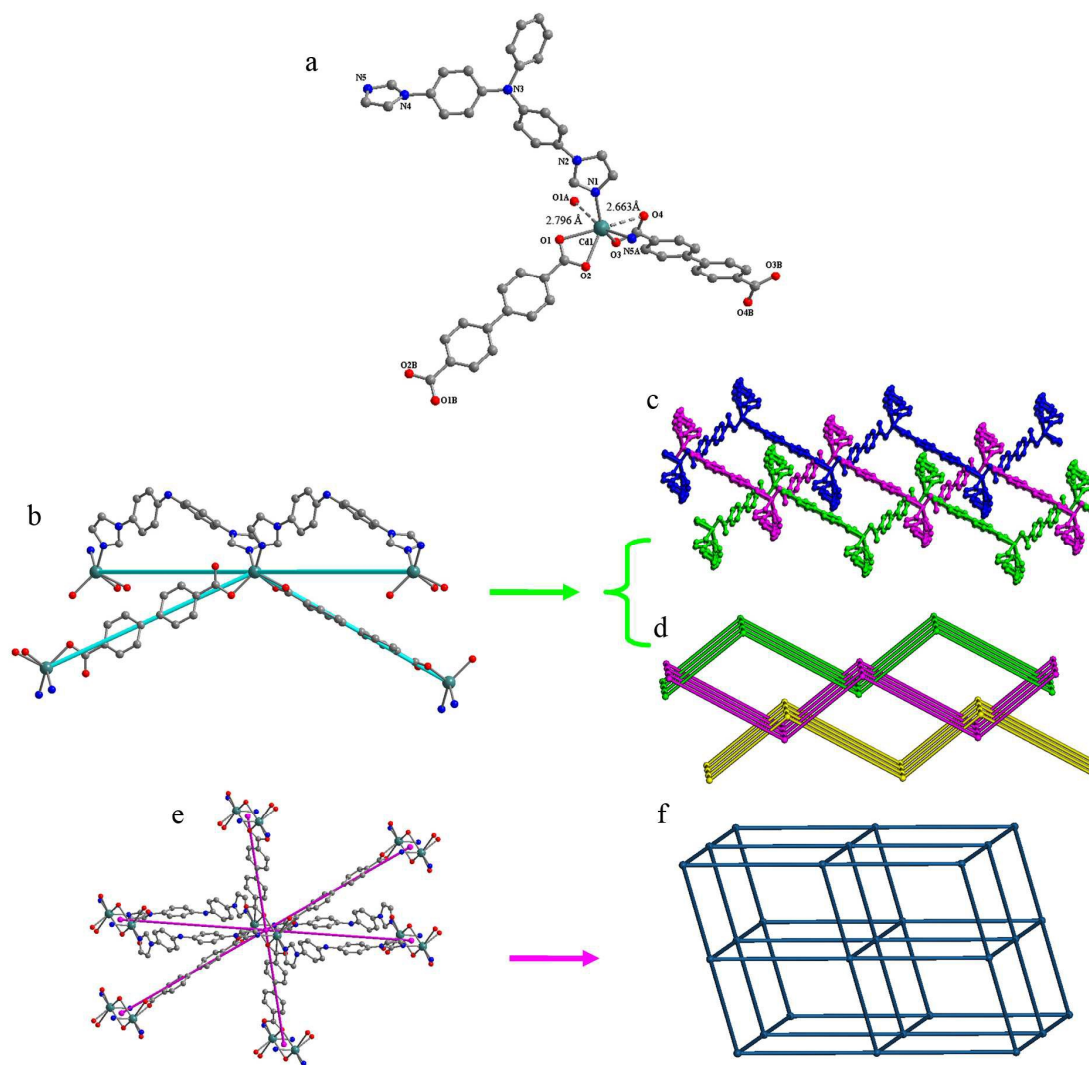


Fig. 6. (a) The coordination environment of Cd(II) atom in **6**. The hydrogen atoms are omitted for clarity. A: x,y,z-1. (b) The perspective view of the 4-connected node (not calculating the weak secondary bonding). (c) and (d) The perspective and schematic views of the 2D→3D polycatenane framework (not calculating the weak secondary bonding). (e) The perspective view of the 6-connected node (calculating the weak secondary bonding). (f) The schematic view of the **pcu** network (calculating the weak secondary bonding). (Noted: the dangling benzyl rings in b, c and e are omitted for clarity)

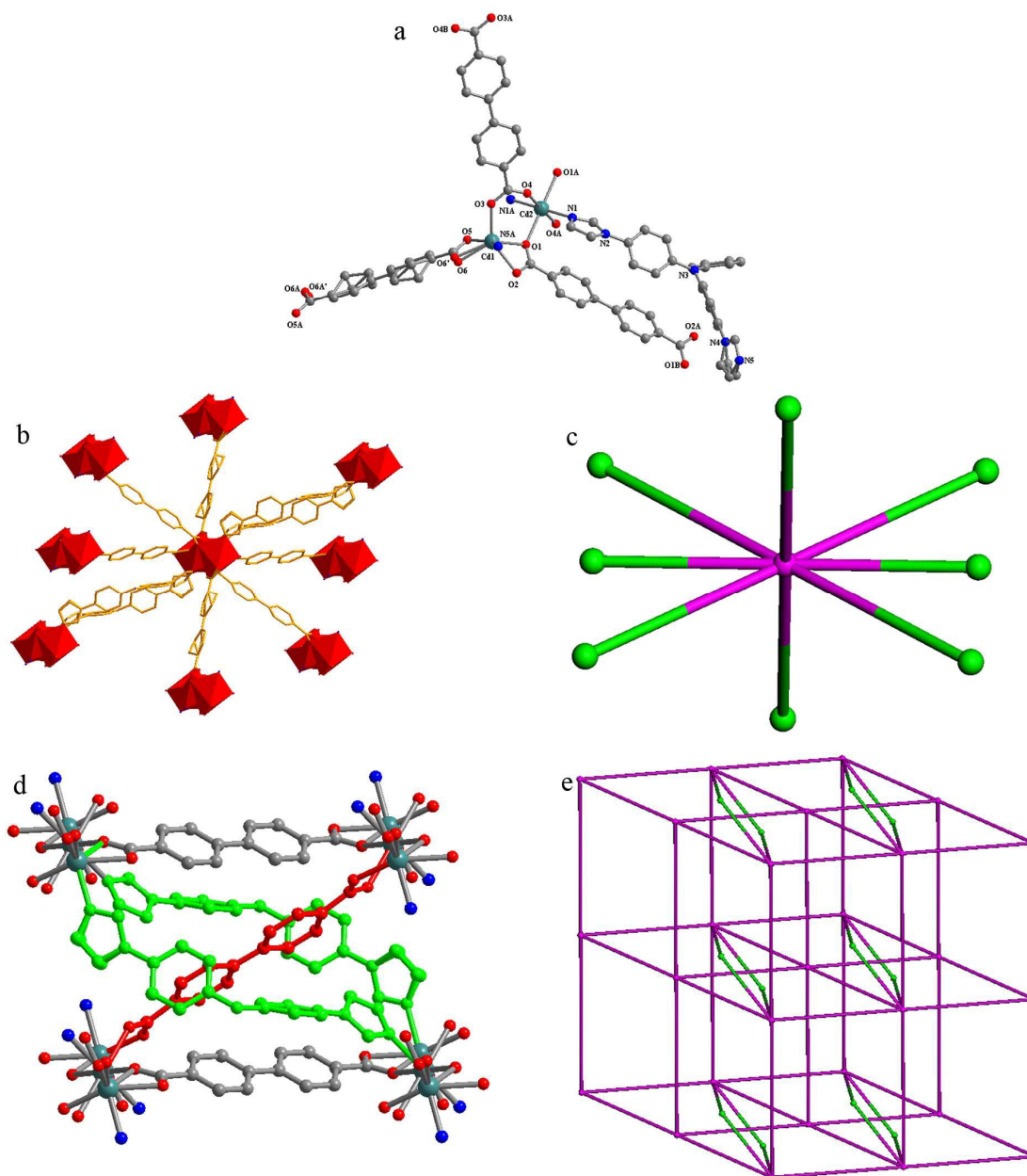


Fig. 7. (a) The coordination environment of Cd(II) atom in 7. The hydrogen atoms are omitted for clarity. A: $-x+1, -y+1, -z$. (b) and (c) The perspective and schematic views of the 8-connected node. (d) The perspective view of the self-penetrating motif in 7. (e) The schematic view of the self-penetrating framework with $(4^{25} \cdot 6^3)$ topology.

5

Table 2. Wavelengths of the emission maxima and excitation (nm) for 1-7 and free ligand bita.

Compound	1	2	3	4	5	6	7	bita
λ_{ex} [nm]	367	369	369	398	359	331	369	369
λ_{em} [nm]	470	397	397	452	390	402	479	398

10

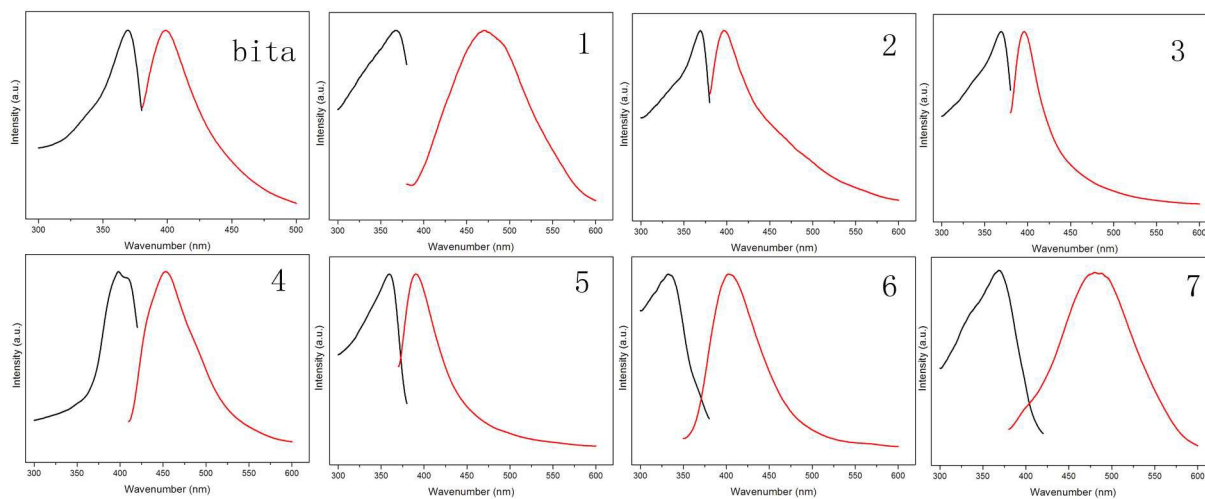
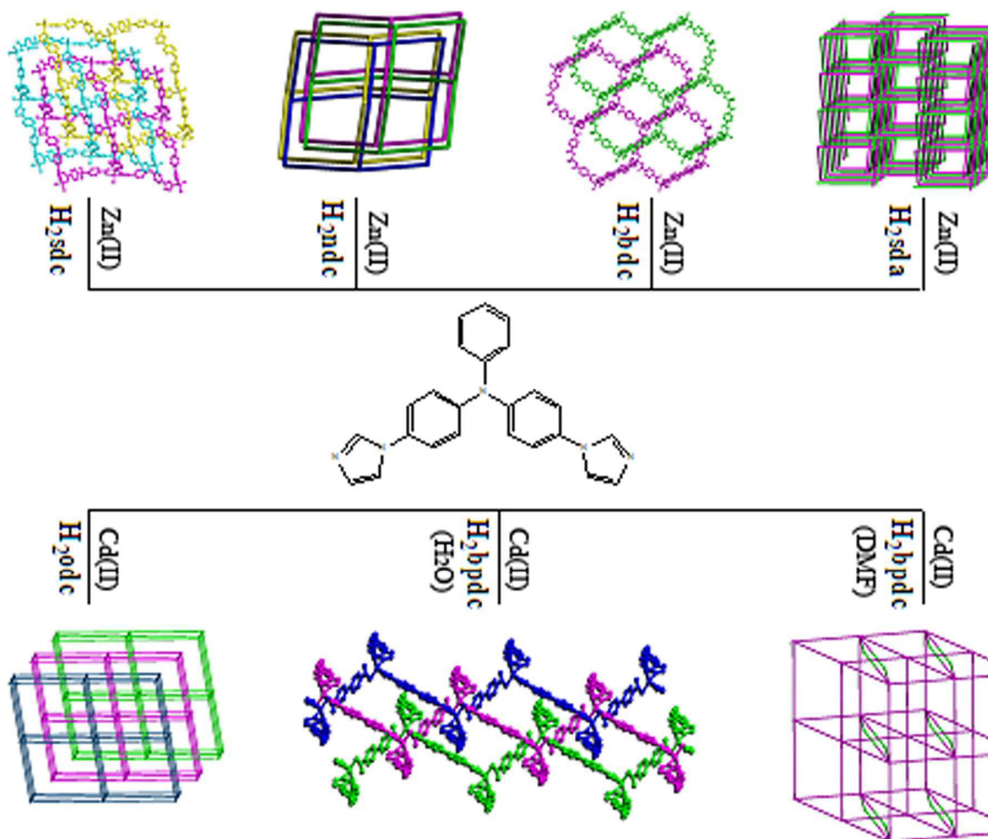


Fig. 8. Emission spectra of 1-7 and bita at room temperature.



Seven entangled mixed-ligand coordination polymers constructed from a triphenylamine-based bisimidazole ligand and versatile carboxylate acids have been hydrothermally synthesized and structurally characterized.